Towards 21-cm intensity mapping with uGMRT wideband observation

Khandakar Md Asif Elahi [1], Somnath Bharadwaj [1], Srijita Pal [2], Abhik Ghosh [3], Sk. Saiyad Ali [4], Samir Choudhuri [5], Arnab Chakraborty [6], Abhirup Datta [7], Nirupam Roy [2], Madhurima Choudhury [8] and Prasun Dutta [9]

[1]Indian Institute of Technology Kharagpur, India; [2]Indian Institute of Science, India; [3]Banwarilal Bhalotia College, India; [4]Jadavpur University, India; [5]Indian Institute of Technology Madras, India; [6]McGill University, Canada; [7]Indian Institute of Technology Indore, India; [8]The Open University of Israel, Israel; [9]IIT (BHU), India

21-cm intensity mapping pipeline

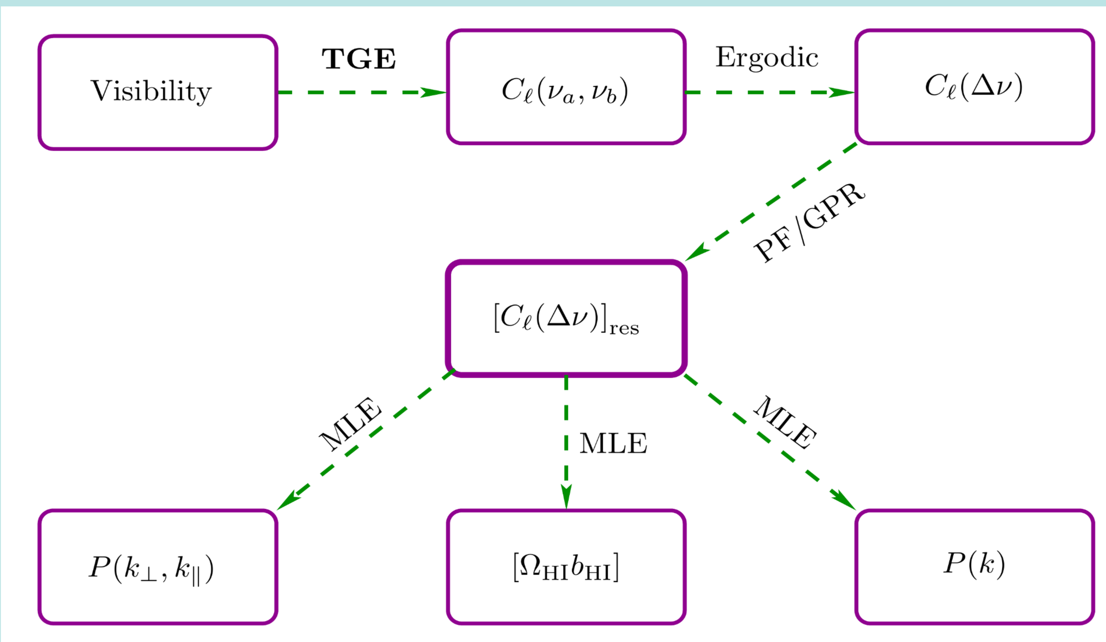

Multi-frequency Angular Power spectrum (MAPS)

$$\delta T_b(\hat{\mathbf{n}},\nu) = \sum_{\ell,m} a_{\ell m}(\nu) Y_\ell^m(\hat{\mathbf{n}})$$

MAPS quantifies the entire second order statistics of the sky signal

$$C_\ell(\nu_a,\nu_b) = \langle a_{\ell m}(\nu_a) a^*_{\ell m}(\nu_b)\rangle$$

$$C_\ell(\nu_a,\nu_b) = C_\ell(|\nu_a-\nu_b|) = C_\ell(\Delta\nu)$$

MAPS and Power Spectrum Related through Fourier Transform

$$P(k_\perp,k_\parallel) = r^2\, r' \int_{-\infty}^{\infty} d(\Delta\nu)\, e^{-ik_\parallel r'\Delta\nu}\, C_\ell(\Delta\nu)$$

Tapered Gridded Estimator (TGE)

$$\mathcal{V}^x_{cg}(\nu_a) = \sum_i \tilde{w}\,(\mathbf{U}_g - \mathbf{U}_i)\, \mathcal{V}^x_i(\nu_a)\, F^x_i(\nu_a) \qquad \mathcal{W}(\theta) = e^{-\theta^2/[f\theta_0]^2}$$

$$\hat{E}_g(\nu_a,\nu_b) = M_g^{-1}(\nu_a,\nu_b)\mathcal{R}e\left[\mathcal{V}^{RR}_{cg}(\nu_a)\mathcal{V}^{*LL}_{cg}(\nu_b) + \mathcal{V}^{LL}_{cg}(\nu_a)\mathcal{V}^{*RR}_{cg}(\nu_b)\right]$$

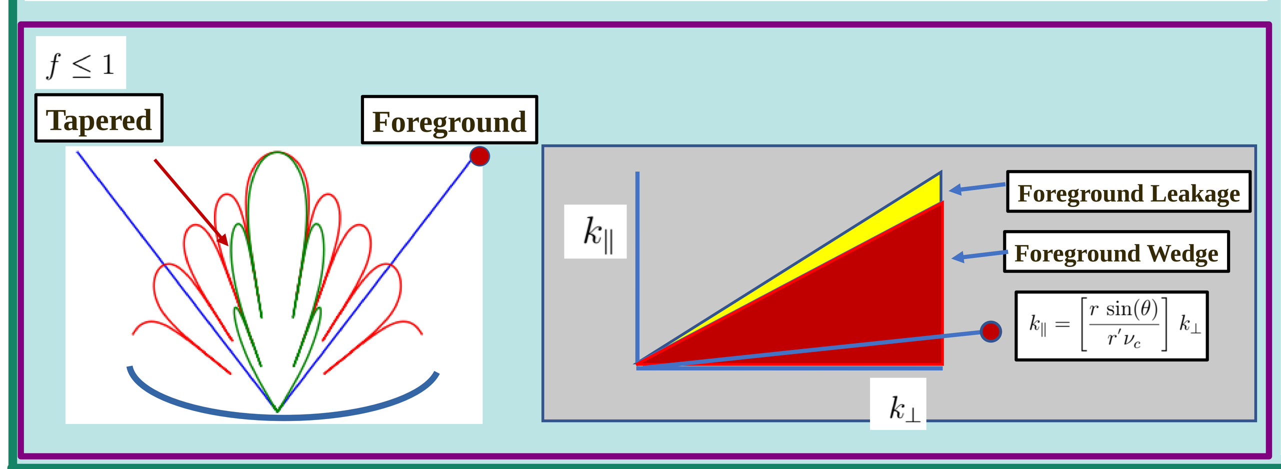

Salient features of TGE

Mitigates widefield foregrounds	suppresses the sidelobe response of the primary beam
Immune to missing frequency channels	Fourier transforms MAPS $C_\ell(\Delta\nu)$ to estimate the power spectrum $P(k_\perp,k_\parallel)$
unbiased estimator	avoids self-correlation of visibilities / cross-polarization
Wideband TGE	Baseline migration Frequency-dependent variation of the primary beam

Power Spectrum

$$C_\ell(\Delta\nu_n) = \sum_m \mathbf{A}_{nm} P(k_\perp,k_{\parallel m}) + [\text{Noise}]_n$$

MLE $$P(k_\perp,k_{\parallel m}) = \sum_n \left[\left(\mathbf{A}^\dagger\mathbf{N}^{-1}\mathbf{A}\right)^{-1}\mathbf{A}^\dagger\mathbf{N}^{-1}\right]_{mn} C_\ell(\Delta\nu_n)$$

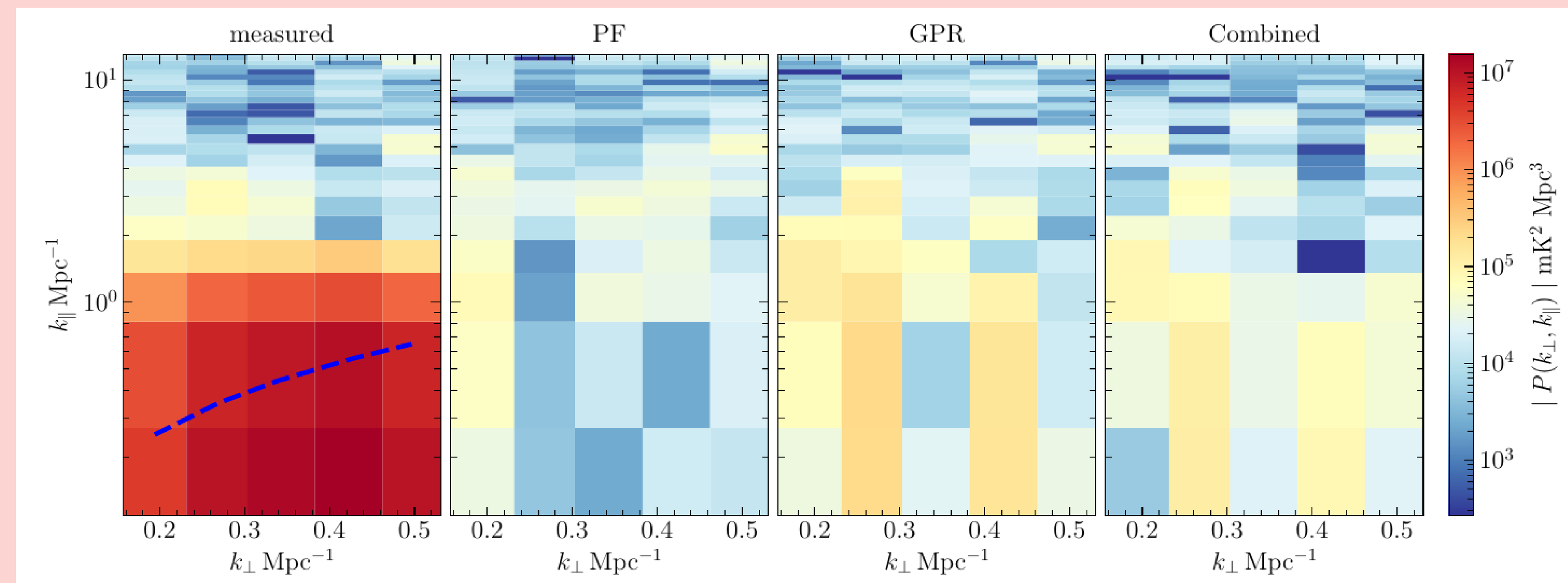

Power Spectrum Statistics

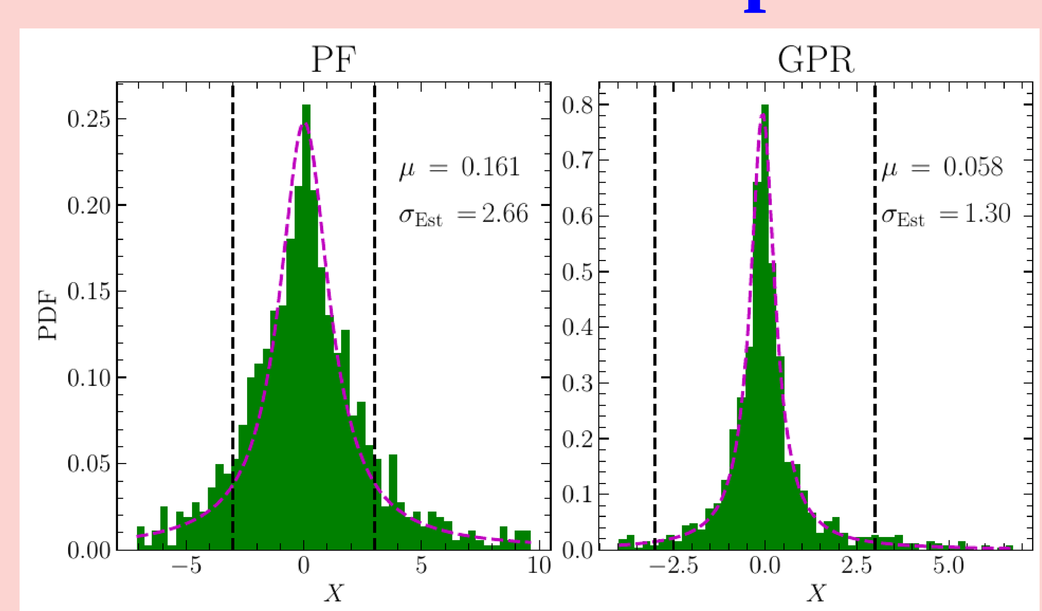

$$X = \frac{P(k_\perp,k_\parallel)}{\delta P_N(k_\perp,k_\parallel)}$$

- Largely symmetric around 0
- Consistent with 0 mean at 95% confidence
- Excess variance

Upper Limits

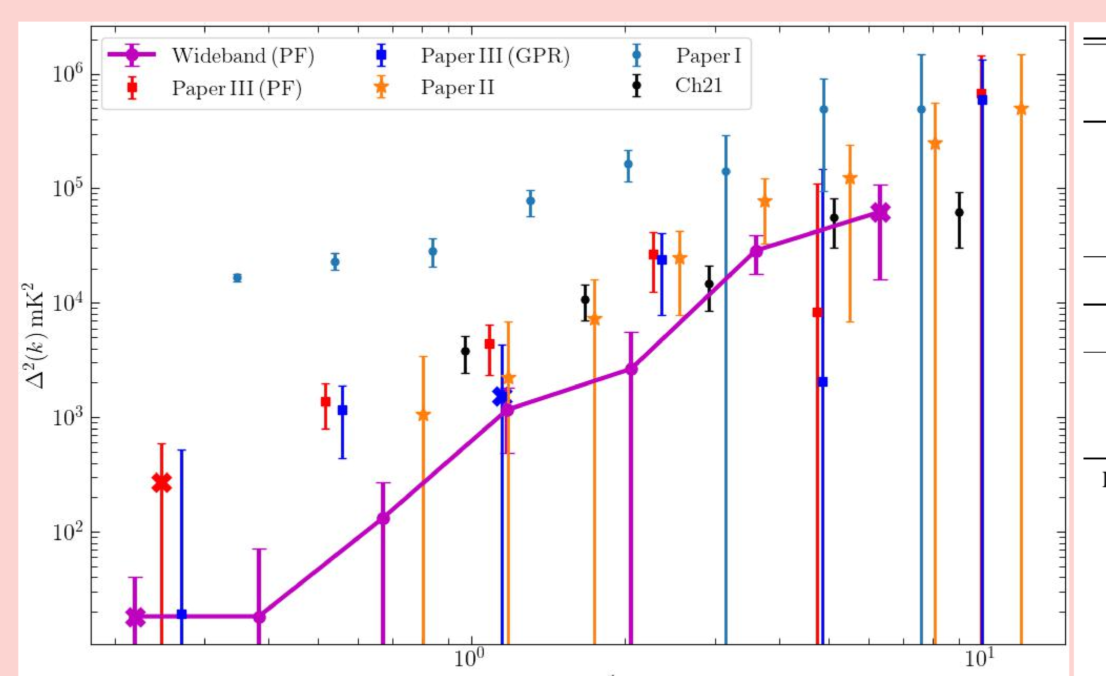

Works	z	k Mpc^{-1}	$\Delta^2_{\rm UL}(k)$ mK^2	$[\Omega_{\rm HI} b_{\rm HI}]_{\rm UL}$
Ch21	1.96 2.19 2.62 3.58	0.99 0.97 0.95 0.99	$(58.57)^2$ $(61.49)^2$ $(60.89)^2$ $(105.85)^2$	0.09 0.11 0.12 0.24
Paper I	2.28	0.35	$(133.97)^2$	0.23
Paper II	2.28	0.80	$(58.67)^2$	0.072
Paper III PF	2.28	0.25	$(18.07)^2$	0.036
Paper III GPR	2.28	0.30	$(24.54)^2$	0.045
Present work				
PF	1.9 – 2.6	**0.22** 0.38	$(\mathbf{4.68})^2$ $(8.48)^2$	**0.010** 0.014
GPR	1.9 – 2.6	0.22 0.40	$(7.56)^2$ $(10.90)^2$	0.016 0.018
Combined	1.9 – 2.6	0.22 **0.38**	$(6.32)^2$ $(\mathbf{6.38})^2$	0.014 **0.011**

Within an order of magnitude of the expected 21-cm signal $\quad [\Omega_{\rm HI} b_{\rm HI}] < 1.01 \times 10^{-2}$

Foreground Removal

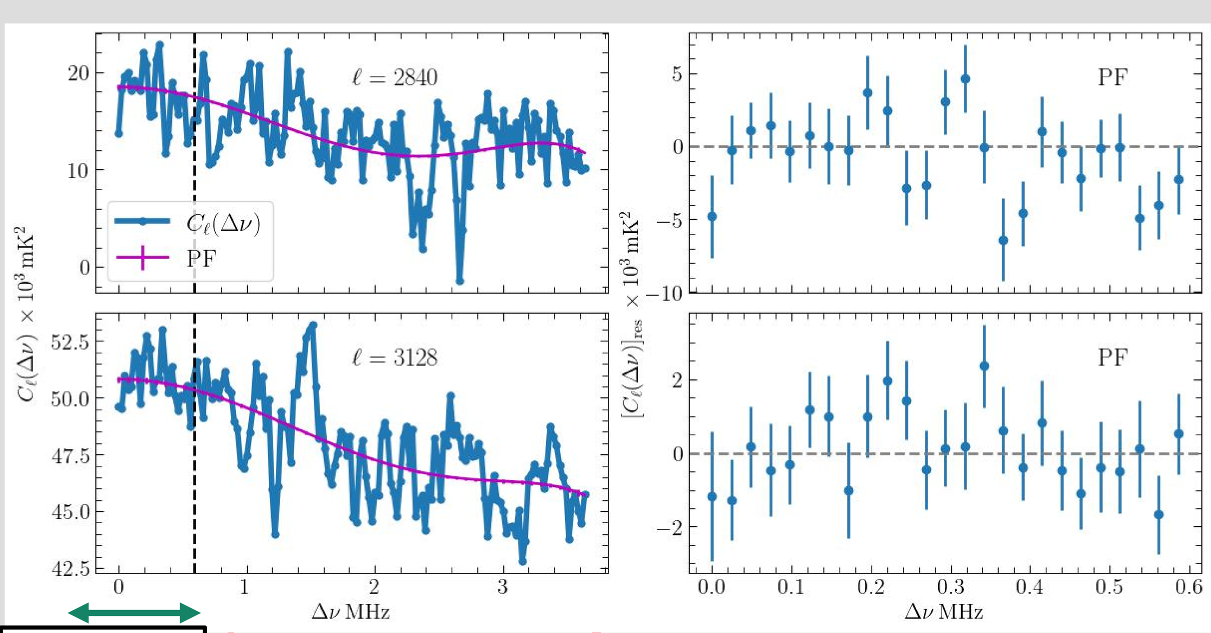

Foreground prediction — Foreground modeling — Residual

Idea: 21-cm signal decorrelates faster than foreground. 21-cm signal is localized within $\Delta\nu \le [\Delta\nu]$

- **Step 1**: **Model** the foregrounds from the range $\Delta\nu > [\Delta\nu]$
  $C_\ell(\Delta\nu) = [C_\ell(\Delta\nu)]_{\rm FG} + [\text{Noise}]$
- **Step 2**: **Predict** the foreground in the range $\Delta\nu \le [\Delta\nu]$
- **Step 3**: **Subtract** the foreground prediction
  $[C_\ell(\Delta\nu)]_{\rm res} = C_\ell(\Delta\nu) - [C_\ell(\Delta\nu)]_{\rm FG}$

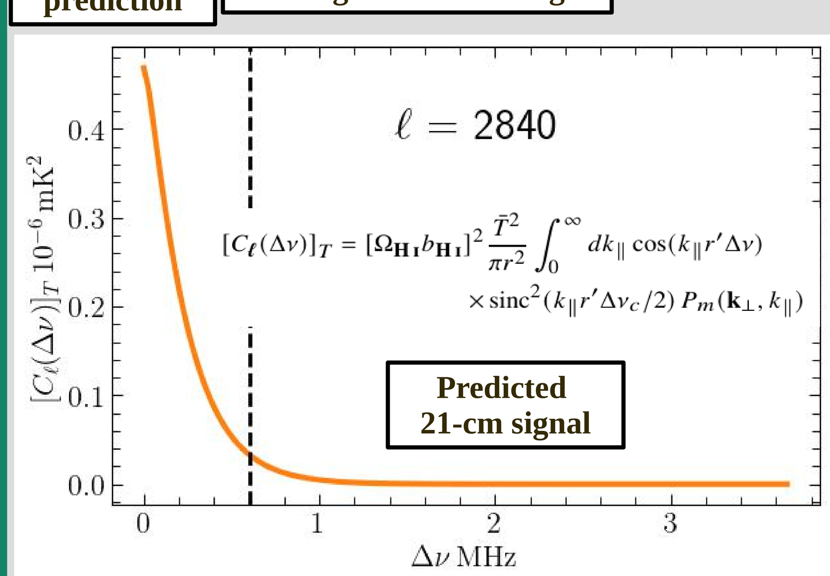

Foreground modeling and predictions

Polynomial Fitting (PF)

$$[C_\ell(\Delta\nu)]_{\rm FG} = \sum_{m=0}^{n} a_{2m}\,(\Delta\nu)^{2m}$$

Gaussian Process Regression (GPR)

$$[C_\ell(\Delta\nu)]_{\rm FG} \sim \mathcal{GP}\,[0,\ k_{\rm FG}(\Delta\nu_m,\Delta\nu_n)]$$

$$k_{\rm FG}(\Delta\nu_m,\Delta\nu_n) = c_1\,(\Delta\nu_m\cdot\Delta\nu_n + b)^P$$

Polynomial kernel

Highlights

TGE	mitigates foregrounds, immune to missing channels, unbiased, capable of wideband analysis
Foreground removal	Removes foregrounds from MAPS [21-cm signal is localized] PF and GPR
Power Spectrum	Free from foregrounds, largely consistent with noise predictions
Upper limit	Observation 25 hours, Bandwidth = 100 MHz (394 – 494 MHz) $\quad [\Omega_{\rm HI} b_{\rm HI}] < 1.01 \times 10^{-2}$
Future directions	✓Longer Observation ✓Other telescopes (CHIME, MeerKAT, SKA) ✓Other frequencies (e.g. EoR)

References

Towards 21-cm intensity mapping at z=2.28 with uGMRT using the tapered gridded estimator

I	Foreground avoidance	Pal S., et al., 2022, MNRAS, 516, 2851	2208.11063
II	Cross-polarization power spectrum	Elahi K. M. A., et al., 2023a, MNRAS, 520, 2094	2301.06677
III	Foreground removal	Elahi K. M. A., et al., 2023b, MNRAS, 525, 3439	2308.08284
IV	Wideband analysis	Elahi K. M. A., et al., 2024, MNRAS (accepted)	2403.06736
Ch21	First multi-redshift limits on post-Epoch of Reionization (post-EoR) 21 cm signal from z = 1.96 - 3.58 using uGMRT	Chakraborty A., et al., 2021, ApJ, 907, L7	2012.04674